

**$B(E2; 0_1^+ \rightarrow 2_1^+)$  values of even-even Sn isotopes**H. Jiang,<sup>1,2,\*</sup> Y. Lei,<sup>2</sup> G. J. Fu,<sup>2</sup> Y. M. Zhao,<sup>2,3,†</sup> and A. Arima<sup>2,4</sup><sup>1</sup>*School of Arts and Sciences, Shanghai Maritime University, Shanghai 201306, China*<sup>2</sup>*Institute of Nuclear, Particle, Astrophysics, and Cosmology, Department of Physics, Shanghai Jiao Tong University, Shanghai 200240, China*<sup>3</sup>*Center of Theoretical Nuclear Physics, National Laboratory of Heavy Ion Accelerator, Lanzhou 730000, China*<sup>4</sup>*Musashi Gakuen, 1-26-1 Toyotamakami Nerima-ku, Tokyo 176-8533, Japan*

(Received 2 August 2012; revised manuscript received 8 October 2012; published 12 November 2012)

The  $2_1^+$  energies and  $B(E2; 0_1^+ \rightarrow 2_1^+)$  values of even-even Sn nuclei with mass numbers between 102 and 130 have been calculated within the framework of the  $SD$ -pair approximation of the nuclear shell model. We employ monopole and quadrupole pairing plus quadrupole-quadrupole interaction with optimized parameters. Good agreement is obtained between the calculated results and experimental data. The robustness of our calculated  $2_1^+$  level and  $E2$  transition rates with respect to different sets of effective charge and different forms of the Hamiltonian is studied.

DOI: [10.1103/PhysRevC.86.054304](https://doi.org/10.1103/PhysRevC.86.054304)

PACS number(s): 21.10.Re, 21.60.Ev, 23.20.Lv, 27.60.+j

**I. INTRODUCTION**

The  $^{100-132}\text{Sn}$  isotopes provide one of the longest chains of semimagic nuclei currently accessible to nuclear structure studies. In recent years, the  $B(E2; 0_1^+ \rightarrow 2_1^+)$  strengths [abbreviated as  $B(E2\uparrow)$ ] of Sn isotopes with even neutron numbers have been of experimental interest [1–8]. Previous experiments [1–7] based on Coulomb excitation showed the measured  $B(E2\uparrow)$  values decrease as the neutron number increases from the midshell nucleus  $^{116}\text{Sn}$  towards the  $N = 82$  shell closure and follow a parabolic behavior, that the  $B(E2\uparrow)$  values below  $^{116}\text{Sn}$  increase first from  $^{116}\text{Sn}$  to  $^{114}\text{Sn}$  and then stay nearly constant within the experimental uncertainties down to  $^{106}\text{Sn}$ . However, the recent measured lifetimes of the first excited  $2^+$  for  $^{112-124}\text{Sn}$  [8] indicated a shallow minimum of the  $B(E2\uparrow)$  values at  $^{116}\text{Sn}$ , followed by a smooth increase up to  $^{112}\text{Sn}$  ( $A < 116$ ) and  $^{120}\text{Sn}$  ( $A > 116$ ), respectively.

A number of theoretical studies of the  $2_1^+$  energies (denoted by  $E_{2_1^+}$ ) and  $B(E2\uparrow)$  values have been carried out in the Sn isotopes, and we summarize these studies as follows. (1) The single- $j$  seniority scheme [9] predicted that the  $E_{2_1^+}$  values are nearly constant and that the  $B(E2\uparrow)$  values follow a smooth parabolic behavior with the maximum at  $^{116}\text{Sn}$ . Recently, a schematic two-level, generalized-seniority study [10] described the observed  $B(E2\uparrow)$  values in Ref. [8], in terms of the order of filling these orbits. (2) The seniority truncated large-scale shell-model (SM) calculations [1, 11, 12] presented parabolic behavior for  $B(E2\uparrow)$  of  $^{102-130}\text{Sn}$ , assuming the  $1d_{5/2}$ ,  $0g_{7/2}$ ,  $1d_{3/2}$ ,  $2s_{1/2}$ , and  $0h_{11/2}$  orbitals. Expanded shell-model calculations [5] showed certain deviations from the symmetric behavior with respect to the midshell but could not reproduce the experimental data. (3) The relativistic quasiparticle random-phase approximation (QRPA) calculations [13, 14] for  $^{100-134}\text{Sn}$  (and the QRPA calculation [15] for  $^{114-134}\text{Sn}$ ) described reasonably the experimental  $B(E2\uparrow)$  values but showed large deviations from the  $E_{2_1^+}$  values.

(4) The quasiparticle-phonon model (QPM) calculations [16] reproduced the  $E_{2_1^+}$  values and the observed deviations of  $B(E2\uparrow)$  from the parabolic behavior along the chain of Sn isotopes. They explained the asymmetry of  $B(E2\uparrow)$  by using evolution of the single-particle energies, polarization of the  $N = Z = 50$  core, interplay between pairing plus quadrupole, and quadrupole pairing interactions.

The purpose of this paper is to perform systematic studies of the  $E_{2_1^+}$  values and  $B(E2\uparrow)$  strengths of even-even  $^{102-130}\text{Sn}$  nuclei from a new perspective. Within the framework of the nucleon pair approximation (NPA) of the shell model, we diagonalize a phenomenological nuclear shell-model Hamiltonian and calculate the low-lying level scheme as well as  $E2$  transition strengths between these levels. Our configuration space is constructed by valence neutron pairs with spins zero and two (denoted by  $S$  and  $D$  pairs, respectively), with respect to the doubly closed shell nuclei  $^{100}\text{Sn}$  and  $^{132}\text{Sn}$  for neutron particles and neutron holes, respectively. For  $2_1^+$  states, the  $SD$ -pair subspace is believed to be a good approximation of the full shell-model space, although the dimension of the NPA wave functions is tremendously smaller than that of the exact shell-model space [17, 18].

This paper is organized as follows. In Sec. II we give a brief introduction to the NPA, including the Hamiltonian, transition operators, and parametrization in our calculations. In Sec. III we present our calculated results including the  $E_{2_1^+}$  values and  $B(E2\uparrow)$  strengths. We also discuss the robustness of our calculated results, in spite of a different set of effective charge, and different forms of the Hamiltonian. The summary and conclusions are given in Sec. IV.

**II. THEORETICAL FRAMEWORK**

The NPA of the shell model can be traced back to the seniority scheme. The generalized seniority [9] and broken-pair approximations [19] have been widely applied to study the structure of single closed-shell nuclei. A number of NPAs have been developed towards the microscopic foundation of the interacting boson models [18]. A technique of constructing

\*huijiang@shmtu.edu.cn

†Corresponding author: ymzhao@sjtu.edu.cn

TABLE I. Adopted single-particle (s.p.) energies (in MeV) for nuclei below the neutron midshell nucleus  $^{116}\text{Sn}$  (denoted by  $\epsilon_j^{(1)}$ ) and at or above  $^{116}\text{Sn}$  (denoted by  $\epsilon_j^{(2)}$ ). They are taken from Refs. [12] and [28], respectively.

$j$	$s_{1/2}$	$d_{3/2}$	$d_{5/2}$	$g_{7/2}$	$h_{11/2}$
$\epsilon_j^{(1)}$	1.550	1.660	0.000	0.080	3.550
$\epsilon_j^{(2)}$	0.332	0.000	1.655	2.434	0.242

symmetry-dictated  $SD$  pairs was invented by Ginocchio in Ref. [20] and further developed by Wu and collaborators [21]. The general framework of the NPA was proposed by Chen in Ref. [22] and refined in Ref. [23]. Theoretical studies have demonstrated that pairs with spins zero (denoted by  $S$ ), two (denoted by  $D$ ), and four (denoted by  $G$ ) play dominant roles in low-lying states [17,18,24]. The NPA was applied to some even-even, odd- $A$ , and odd-odd nuclei with  $A \sim 80, 130$ , and 210 in recent years [25–30].

The Hamiltonian  $H$  that we take is as follows:

$$H = \sum_j \epsilon_j C_j^\dagger C_j + G_0 \mathcal{P}^{(0)\dagger} \cdot \mathcal{P}^{(0)} + G_2 \mathcal{P}^{(2)\dagger} \cdot \mathcal{P}^{(2)} + \kappa Q \cdot Q, \quad (1)$$

where  $\epsilon_j$  is the single-particle energy and  $C_j^\dagger$  and  $C_j$  are single-particle creation and annihilation operators, respectively. The adopted single-particle energies in our calculations for nuclei below (and at or above) the neutron midshell nucleus  $^{116}\text{Sn}$  (denoted by  $\epsilon_j^{(1)}$  and  $\epsilon_j^{(2)}$ , respectively) are shown in Table I. They are taken from Refs. [12,28], respectively. We treat nuclei with mass number  $A < 116$  as valence neutrons in the 50-82 shell, assume  $\epsilon_j^{(1)}$  as the single-particle energies, and treat nuclei with  $A \geq 116$  as neutron holes with  $\epsilon_j^{(2)}$  as the single-particle energies:

$$\begin{aligned} \mathcal{P}^{(0)\dagger} &= \sum_j \frac{\sqrt{2j+1}}{2} (C_j^\dagger \times C_j^\dagger)_0^{(0)}, \\ \mathcal{P}^{(2)\dagger} &= \sum_{jj'} q(jj') (C_j^\dagger \times C_{j'}^\dagger)_M^{(2)}, \\ Q &= \sum_{jj'} q(jj') (C_j^\dagger \times \tilde{C}_{j'})_M^{(2)}. \end{aligned} \quad (2)$$

$G_0$ ,  $G_2$ , and  $\kappa$  of Eq. (1) are the two-body interaction parameters for monopole and quadrupole pairing interactions and quadrupole-quadrupole interactions between valence neutrons. They are adjusted based on the experimental  $E_{2_1^+}$  and  $B(E2\uparrow)$  values for  $A < 116$  and  $A \geq 116$ , respectively, as shown in Table II. The unit of  $G_0$  is MeV, and the

TABLE II. Parameters  $G_0$ ,  $G_2$ , and  $\kappa$  of our two-body interactions. The unit of  $G_0$  is MeV; the units of  $G_2$  and  $\kappa$  are  $\text{MeV}/r_0^4$ ,  $r_0^2 = 1.012A^{1/3} \text{ fm}^2$ .

Nucleus	$G_0$	$G_2$	$\kappa$
$A < 116$	-0.180	-0.018	-0.039
$A \geq 116$	-0.131	-0.013	-0.034

units of  $G_2$  and  $\kappa$  are  $\text{MeV}/r_0^4$ ,  $r_0^2 = 1.012A^{1/3} \text{ fm}^2$ . Here  $q(jj') = \frac{(-)^{j'-1/2}}{\sqrt{20\pi}} \hat{j} \hat{j}' C_{j1/2, j'-1/2}^{20} \langle nl|r^2|nl' \rangle$ , where  $C_{j1/2, j'-1/2}^{20}$  is the Clebsch-Gordan coefficient and the matrix elements  $\langle nl|r^2|nl' \rangle$  are the same as in Ref. [28].

The  $E2$  transition operator is defined as follows.  $T(E2) = e_v Q$ , where  $e_v$  is the effective charge of valence neutrons. In our calculations we use different effective charges,  $e_v = 1.28e$  for  $A < 116$  and  $-0.95e$  for  $A \geq 116$ . The effective charge for  $A < 116$  regions is larger than that for  $A \geq 116$ , due to the different character of core excitations towards  $N = Z = 50$  and  $N = 82$  shell closure of the Sn isotopic chain studied in Refs. [3,12]. The electric quadrupole moment is defined by  $Q = \sqrt{\frac{16\pi}{5}} T(E2)$ .

Because we focus on the  $E_{2_1^+}$  value and  $B(E2\uparrow)$  strength, our pair space is constructed by  $SD$  nucleon pairs, with respect to the doubly closed shell nucleus  $^{100}\text{Sn}$  for  $A < 116$  and  $^{132}\text{Sn}$  for  $A \geq 116$ , respectively. We have made comparisons between the calculated results of the  $SD$ -pair subspace and those with larger configurations, for example, inclusion of  $G$  pairs for the ground state, and the first excited states. We find that the effect outside the  $SD$  space is negligible (the relative deviation is  $\sim 0.001$ ). For example, our calculated  $B(E2\uparrow)$  value for  $^{124}\text{Sn}$  is 0.1730 ( $e^2 b^2$ ) in the  $SD$  configuration space and 0.1737 ( $e^2 b^2$ ) in the  $SDG$  configuration space. As in Refs. [27,28], we use the BCS pairs as our  $S$  pair. The  $D$  pair is obtained by using the commutator  $D^\dagger = \frac{1}{2}[Q, S^\dagger]$  [19].

### III. CALCULATED RESULTS

Our calculated results of  $E_{2_1^+}$  and  $B(E2\uparrow)$  are presented in Fig. 1 using solid squares in blue [gray]. The experimental  $E_{2_1^+}$  values and  $B(E2\uparrow)$  strengths of  $^{106,108}\text{Sn}$ ,  $^{110}\text{Sn}$ ,  $^{112-124}\text{Sn}$ , and  $^{126-130}\text{Sn}$  are taken from Refs. [1,4,5,8,31], respectively. As is well known, the ground states of these even-even Sn isotopes are dominated by  $S$  pairs, and the  $2_1^+$  states are dominated by the  $|D(S)^{N_v-1}\rangle$ . Our calculated results are consistent with this description. For comparison, we also show the results of other theoretical works (the SM, the QPM, and the RQRPA) taken from Refs. [12,13,16], respectively.

One sees in Fig. 1(a) that our calculated  $E_{2_1^+}$  levels agree well with the experimental ones. For the  $B(E2\uparrow)$  in Fig. 1(b), our results satisfactorily reproduce the following two characteristics: the shallow minimum at  $^{116}\text{Sn}$  and the asymmetry for even-even Sn isotopes with  $A < 116$  and  $A \geq 116$ . For  $A \geq 122$ , our  $B(E2\uparrow)$  values deviate from the experimental data by approximately 0.01–0.04  $e^2 b^2$ . In order to investigate whether we can obtain better agreement with experimental data by expanding our model space, we have performed calculations by adjusting the interactions in Table II, or considering more non- $S$  pairs (e.g.,  $G$  pair). However, this deviation is found to be very robust. Therefore, it will be interesting in the future to study the origin of this deviation (although very small). In Fig. 1, one also notices that an increase in  $E_{2_1^+}$  values around  $^{116}\text{Sn}$  well corresponds to the observed minimum of  $B(E2\uparrow)$ .

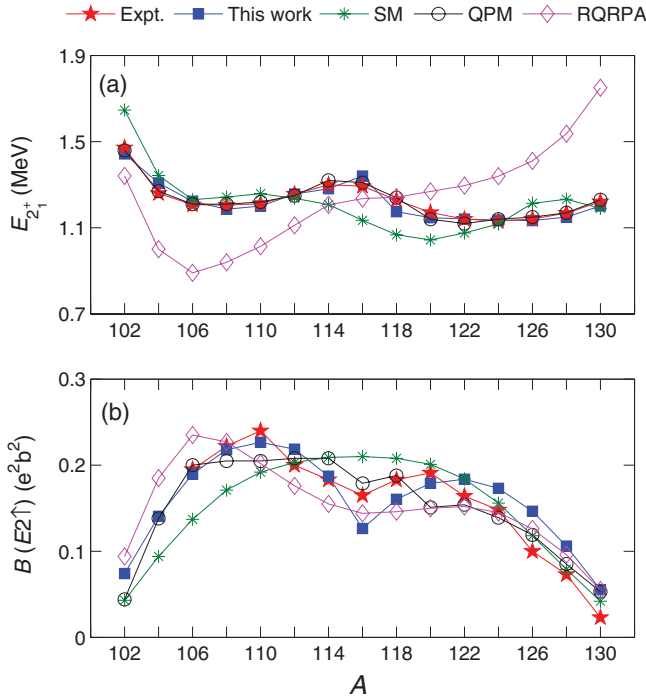


FIG. 1. (Color online) The  $E_{2_1^+}$  and  $B(E2\uparrow)$  values of even-even  $^{102-130}\text{Sn}$  nuclei. The experimental  $E_{2_1^+}$  values and  $B(E2\uparrow)$  strengths of  $^{106,108}\text{Sn}$ ,  $^{110}\text{Sn}$ ,  $^{112-124}\text{Sn}$ , and  $^{126-130}\text{Sn}$  are taken from Refs. [1,4,5,8,31], respectively. Our results are shown as solid squares in blue [gray], with effective charges  $e_v = 1.28e$  for  $A < 116$  and  $-0.95e$  for  $A \geq 116$ . Results of other theoretical works (the SM, the QPM, and the RQRPA) are taken from Refs. [12,13,16], respectively.

In Fig. 2 we present the  $SD$  pair structure coefficients. One sees that the  $SD$  pairs consist essentially of two valence neutrons in the  $g_{7/2}$  and  $d_{5/2}$  orbits (single-particle energies  $\epsilon_j^{(1)}$ ) for  $A < 116$  and of neutron holes in the  $h_{11/2}$ ,  $d_{3/2}$ , and  $s_{1/2}$  orbits (single-particle energies  $\epsilon_j^{(2)}$ ) for  $A \geq 116$ . This picture is more apparent if one investigates the fillings of the single-particle orbits in the 50-82 shell. In Fig. 3 we present the occupation number  $n_j$  in the  $j = 1/2^+, 3/2^+, 5/2^+, 7/2^+$ , and  $11/2^-$  orbits. Here  $n_j$  is the expectation value of valence neutrons in these five orbits for  $A < 116$  or that of neutron holes for  $A \geq 116$ . From Fig. 3, one sees that for nuclei with  $N$  below 66 the favored orbits are  $g_{7/2}$  and  $d_{5/2}$ , and the low-lying states of nuclei with  $N \geq 66$  can be described in terms of neutron holes in the  $h_{11/2}$ ,  $d_{3/2}$ , and  $s_{1/2}$  orbits. For both the ground state and the first  $2_1^+$  state of  $^{116}\text{Sn}$ , the three single-particle (holelike) levels ( $h_{11/2}$ ,  $d_{3/2}$ , and  $s_{1/2}$ ) are almost fully occupied by neutron holes (because  $n_j \simeq 2j + 1$ ). The effective number of valence neutrons (holes) that contribute to the collective motion is smaller than it is based on the counting scheme of the nearest magic numbers, 50 and 82. This is a feature of the subshell. In Ref. [7] it was also pointed out that there seems to be a soft closed subshell at  $N = 64$  for the Sn isotopic chain; for  $^{102-114}\text{Sn}$ , the  $2_1^+$  state is dominated by the neutrons in the  $\nu d_{5/2}$  and  $\nu g_{7/2}$  orbits.

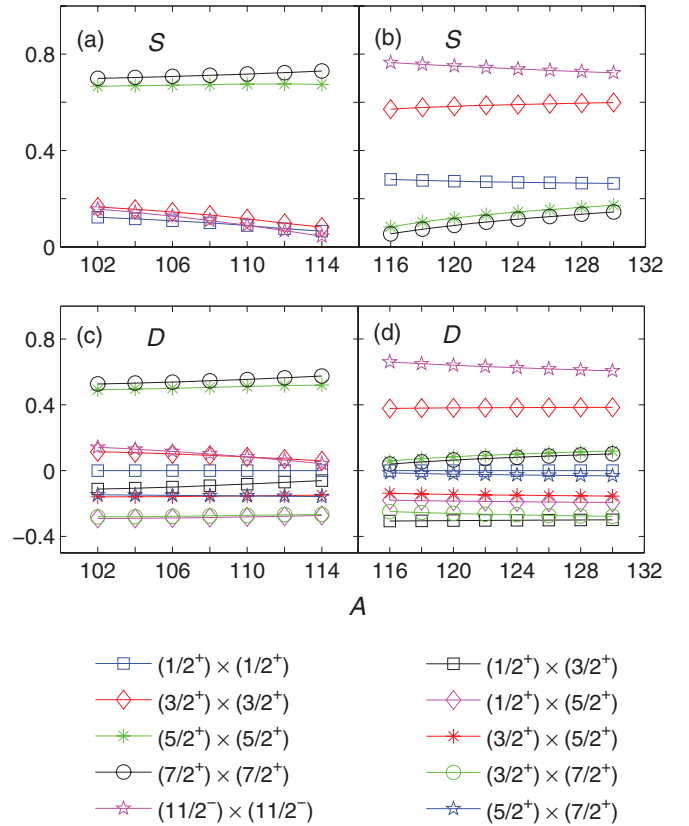


FIG. 2. (Color online) The  $S$  and  $D$  pair structure coefficients of even-even Sn isotopes. For  $A < 116$  ( $A \geq 116$ ), the pairs are given by two valence neutrons (neutron holes) in the five orbits with single-particle energies  $\epsilon_j^{(1)}$  ( $\epsilon_j^{(2)}$ ).

The soft subshell effect at  $N = 64$  would give a shallow minimum in  $B(E2\uparrow)$  of Sn isotopes at  $A = 114$  other than  $A = 116$  (which was observed to have the minimum  $B(E2)$  value [8]), if the same effective charge of valence neutrons were assumed for all nuclei. The observed minimum of  $B(E2\uparrow)$  at  $A = 116$  is given by an interplay between the  $N = 64$  subshell and the smaller effective charges for nuclei with  $A \geq 116$ , which is based on the asymmetry of  $B(E2)$  values, as discussed below.

We now come to the asymmetry of  $B(E2\uparrow)$  strengths for  $A < 116$  and  $A \geq 116$ . Apparently, the  $B(E2\uparrow)$  value here is sensitive to the effective charge of valence neutrons. In Fig. 4, we present the  $B(E2\uparrow)$  values calculated by using effective charge in the NPA ( $e_v = 1.28e$  for  $A < 116$  and  $-0.95e$  for  $A \geq 116$ ) and the QPM (effective charge =  $1.05e$  for protons and  $0.05e$  for neutrons), denoted by the NPA-1 and QPM-1. For  $A < 116$  the resultant effective charge is larger. This implies larger core polarizations due to particle-hole excitations for nuclei with  $A < 116$  and a different character of core excitations towards  $N = Z = 50$  and  $N = 82$  shell closure, as pointed out in Refs. [3,12]. The QPM analysis supports the same picture. In the  $2_1^+$  states of  $^{106-118}\text{Sn}$ , configurations of the  $N = Z = 50$  core (in particular, proton degree of freedom) contribute to the  $B(E2)$  values. This leads to a larger effective charge of valence neutrons for these nuclei.

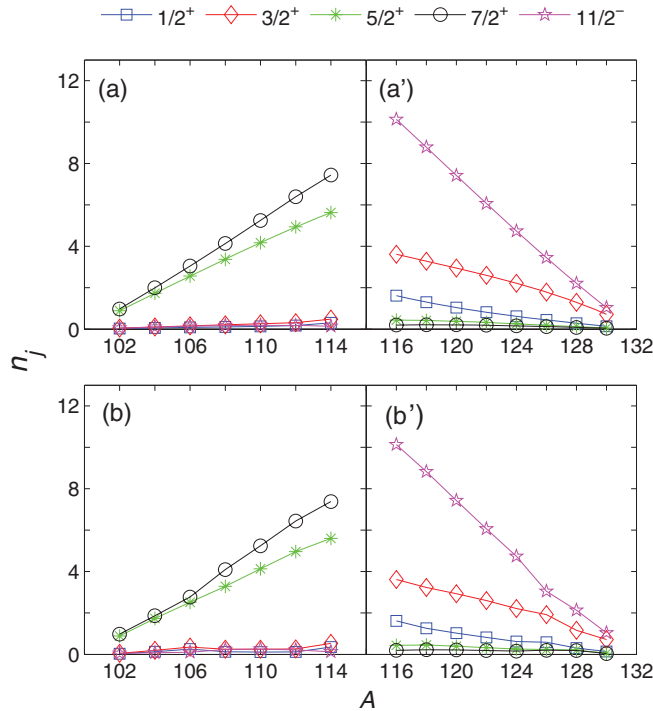


FIG. 3. (Color online) The expectation value of occupation number  $n_j$  in the  $1/2^+$ ,  $3/2^+$ ,  $5/2^+$ ,  $7/2^+$ , and  $11/2^-$  orbits versus mass number  $A$ . Panels (a) and (a'): the spin-zero ground state. Panels (b) and (b'): the first excited state with spin 2. In panels (a) and (b) we present the number of valence neutrons ( $A < 116$ ), and in panels (a') and (b') we present the number of neutron holes ( $A \geq 116$ ) in the corresponding single-particle orbits.

For comparison, we present calculated  $B(E2\uparrow)$  in the NPA by assuming  $e_v = e$  for  $A < 116$  and  $-e$  for  $A \geq 116$ , denoted by NPA-2. The QPM-2 assumes bare charge (i.e.,  $e$  for protons and zero for neutrons). One sees very large deviations from experimental  $B(E2)$  values in both the NPA-2 and QPM-2 calculations if one assumes  $e_v = e$  for  $A < 116$  and  $-e$  for  $A \geq 116$ .

Here it would be useful to compare our effective charges in this work with those in some previous studies. In the QPM calculations excitations of both protons (in the core) and neutrons are considered. The effective charges are close to the bare charges of protons ( $e$ ) and neutrons (zero charge) [16]. In the large-scale shell-model calculations, the effective charge is  $1.5e$  for protons and  $0.5e$  for neutrons if one assumes  $^{90}\text{Zr}$  as the inert core, or  $1-1.5e$  for valence neutrons if one assumes  $^{100}\text{Sn}$  as the inert core, for the Sn isotopes of mass number  $A$  below 116 [12]; the effective charge is  $-0.7-0.8e$  for neutron holes if one assumes  $^{132}\text{Sn}$  as the closed-shell core for Sn isotopes of mass larger than 116 [32]. Therefore, the effective charge that we use in this work is compatible with those in previous studies. The value of effective charge depends on the model space considered in the calculation.

We finally investigate the robustness of our results with respect to different forms of the Hamiltonians. In Fig. 5 we take three forms of the Hamiltonian.  $H-1$  includes only the spherical single-particle energy term and the residual

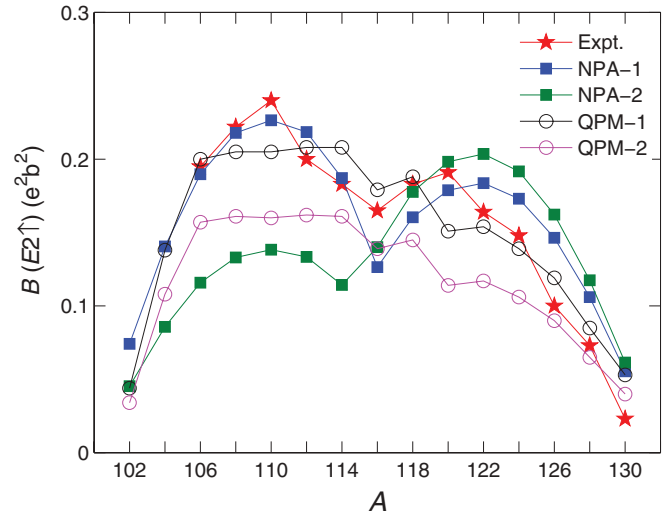


FIG. 4. (Color online) The  $B(E2\uparrow)$  values with effective and bare charges. NPA-1 and NPA-2 are our results with effective charges ( $e_v = 1.28e$  for  $A < 116$  and  $-0.95e$  for  $A \geq 116$ ) and equal effective charges ( $e_v = e$  for  $A < 116$  and  $-e$  for  $A \geq 116$ ), respectively. QPM-1 and QPM-2 are results using effective charges ( $1.05e$  for protons and  $0.05e$  for neutrons) and bare charges ( $e$  for protons and zero charge for neutrons) in Ref. [16].

monopole pairing interaction between valence neutrons.  $H-2$  further considers the residual quadrupole pairing interaction based on  $H-1$ , and  $H-3$  considers the quadrupole-quadrupole interaction based on  $H-2$ . There are two interesting remarks to make, according to the results shown in Fig. 5. (1) In  $H-1$ , the observed  $B(E2\uparrow)$  strengths can be well reproduced, but the calculated  $E_{2_1^+}$  values have large deviations from the experimental ones. This has been already discussed by the results of a schematic two-level, generalized-seniority calculations in Ref. [10], whose Hamiltonian includes only the spherical single-particle energy term and monopole pairing interaction. (2) The interplay of quadrupole pairing and quadrupole-quadrupole interaction is important to reproduce both the energies and the transition strengths. The contributions from quadrupole pairing and quadrupole-quadrupole interaction to the  $B(E2\uparrow)$  values cancel out each other, as shown in Fig. 5(b).  $B(E2\uparrow)$  decreases (or increases) if only the quadrupole pairing (or the quadrupole-quadrupole interaction) is added to  $H-1$ . This behavior was discussed in Ref. [24] for the ground-state energy of nucleons in a single- $j$  shell. Reference [16] also pointed out the quenching and smoothing effect of the quadrupole pairing for the Sn isotopes. As for the  $E_{2_1^+}$  values in Fig. 5(a), only when both the quadrupole pairing and quadrupole-quadrupole interactions are added ( $H-3$ ) can we obtain a satisfactory agreement with the experimental data.

#### IV. SUMMARY

In this paper we calculate the  $E_{2_1^+}$  and  $B(E2\uparrow)$  values of even-even Sn isotopes with mass numbers from 102 to 130 within the  $SD$ -pair approximation of the nuclear shell model. The contribution from configurations beyond the  $SD$  nucleon

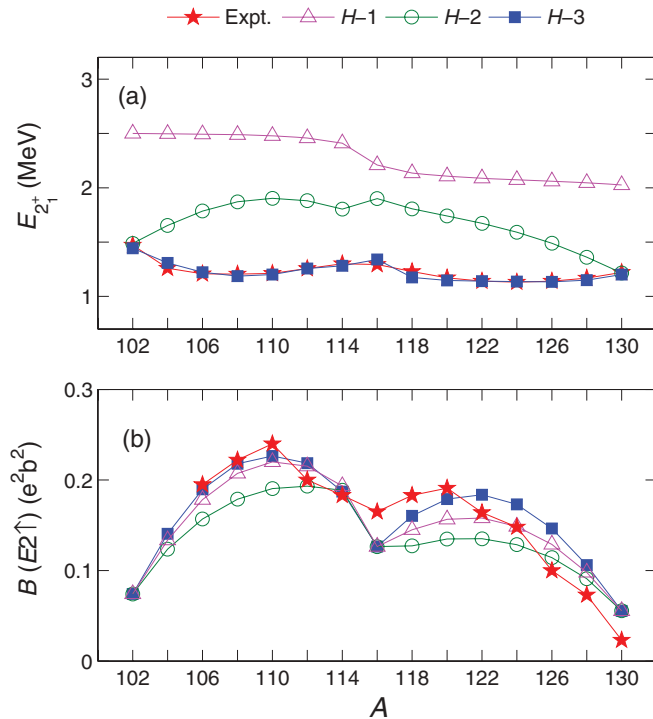


FIG. 5. (Color online) The  $E_{2_1^+}$  and  $B(E2\uparrow)$  values of the present work with different forms of the Hamiltonian (denoted as  $H-1$ ,  $H-2$ , and  $H-3$ , respectively).  $H-1$  includes the spherical single-particle energy term and the residual monopole pairing interaction between valence neutrons.  $H-2$  further considers the residual quadrupole pairing interaction to the  $H-1$ .  $H-3$  adds the quadrupole-quadrupole interaction to the  $H-2$ . The value of effective charge is  $e_v = 1.28e$  for  $A < 116$  and  $-0.95e$  for  $A \geq 116$ .

pairs is very small for the ground and the first excited states of even-even Sn isotopes and is thus neglected in our calculation. We take the phenomenological shell-model Hamiltonian, which includes the single-particle energy term, monopole and quadrupole pairing, and quadrupole-quadrupole interaction between valence neutrons. In order to describe the  $B(E2\uparrow)$  values properly, we use two sets of single-particle energies,

two-body interaction parameters, and effective charges for  $A < 116$  and  $A \geq 116$ . Our calculated results satisfactorily reproduce the observed  $E_{2_1^+}$  levels, the asymmetry of  $B(E2\uparrow)$  for  $A < 116$  and  $A \geq 116$ , and a shallow minimum of  $B(E2\uparrow)$  at  $^{116}\text{Sn}$ .

Our calculation shows that when the neutron number is around 64, the  $g_{7/2}$  and  $d_{5/2}$  orbits are almost fully occupied, while the  $h_{11/2}$ ,  $d_{3/2}$ , and  $s_{1/2}$  orbits are nearly unoccupied. This is given by the soft subshell around neutron number  $N = 64$ . Therefore, the effective valence neutron numbers for  $A \simeq 114$  are smaller than they are based on the counting scheme considering the nearest magic numbers, 50 and 82. On the other hand, the asymmetry of  $B(E2)$  values requires smaller effective charge of valence neutrons for  $A \geq 116$ , which further reduces the calculated  $B(E2\uparrow)$  value for  $A = 116$  and leads to the shallow minimum of  $B(E2\uparrow)$  values at  $A = 116$  instead of  $A = 114$ . In other words, the shallow minimum of  $E2$  transition rates at  $A \simeq 116$  of even-even Sn isotopes is given by the interplay between the soft  $N = 64$  subshell and different core polarization of the  $^{100}\text{Sn}$  and  $^{132}\text{Sn}$  (i.e., different effective charges for nuclei with  $A \leq 114$  and  $A \geq 116$ ).

The robustness of our calculated  $E_{2_1^+}$  and  $B(E2\uparrow)$  with respect to different effective charges and different forms of the Hamiltonian is studied. If one assumed a Hamiltonian that includes only the single-particle energy term plus the monopole pairing term, the observed  $B(E2\uparrow)$  strengths could be well reproduced, but the calculated  $E_{2_1^+}$  values would have large deviations from the experimental results. The interplay of quadrupole pairing and quadrupole-quadrupole interaction is shown to be important to reproduce both the energies and the transition strengths.

#### ACKNOWLEDGMENTS

We thank the National Natural Science Foundation of China (Grants No. 11225524, 10975096 and 11145005), the 973 Program of China (Grant No. 2013CB834401), and the Science and Technology Committee of Shanghai City (Grant No. 11DZ2260700) for financial support.

- [1] D. C. Radford, C. Baktash, J. R. Beene *et al.*, *Nucl. Phys. A* **746**, 83 (2004).
- [2] D. C. Radford, C. Baktash, C. J. Barton *et al.*, *Nucl. Phys. A* **752**, 264 (2005).
- [3] J. Cederkäll, A. Ekström, C. Fahlander *et al.*, *Phys. Rev. Lett.* **98**, 172501 (2007).
- [4] C. Vaman, C. Andreoiu, D. Bazin *et al.*, *Phys. Rev. Lett.* **99**, 162501 (2007).
- [5] A. Ekström, J. Cederkäll, C. Fahlander *et al.*, *Phys. Rev. Lett.* **101**, 012502 (2008).
- [6] P. Doornenbal, P. Reiter, H. Grawe *et al.*, *Phys. Rev. C* **78**, 031303(R) (2008).
- [7] R. Kumar, P. Doornenbal, A. Jhingan *et al.*, *Phys. Rev. C* **81**, 024306 (2010).
- [8] A. Jungclaus, J. Walker, J. Leske *et al.*, *Phys. Lett. B* **695**, 110 (2011).
- [9] I. Talmi, *Nucl. Phys. A* **172**, 1 (1972); *Simple Models of Complex Nuclei* (Harwood Academic, Chur, Switzerland, 1993).
- [10] I. O. Morales, P. Van Isacker, and I. Talmi, *Phys. Lett. B* **703**, 606 (2011).
- [11] S. Raman, C. W. Nestor, and P. Tikkanen, *At. Data Nucl. Data Tables* **78**, 1 (2001).
- [12] A. Banu, J. Gerl, C. Fahlander *et al.*, *Phys. Rev. C* **72**, 061305(R) (2005).
- [13] A. Ansari, *Phys. Lett. B* **623**, 37 (2005).
- [14] A. Ansari and P. Ring, *Phys. Rev. C* **74**, 054313 (2006).
- [15] J. Terasaki, *Nucl. Phys. A* **746**, 583 (2004).
- [16] N. L. Iudice, Ch. Stoyanov, and D. Tarpanov, *Phys. Rev. C* **84**, 044314 (2011).
- [17] Y. Lei, Z. Y. Xu, Y. M. Zhao, and A. Arima, *Phys. Rev. C* **80**, 064316 (2009); **82**, 034303 (2010), and references therein.

- [18] F. Iachello and A. Arima, *The Interacting Boson Model* (Cambridge University Press, Cambridge, 1987); F. Iachello and I. Talmi, *Rev. Mod. Phys.* **59**, 339 (1987).
- [19] K. Allart, E. Boeker, G. Bonsignori, M. Saroia, and Y. K. Gambhir, *Phys. Rep.* **169**, 209 (1988).
- [20] J. N. Ginocchio, *Ann. Phys.* **126**, 234 (1980).
- [21] C. L. Wu, D. H. Feng, X. G. Chen, J. Q. Chen, and M. W. Guidry, *Phys. Rev. C* **36**, 1157 (1987); C. L. Wu, D. H. Feng, and M. Guidry, *Adv. Nucl. Phys.* **21**, 227 (1994).
- [22] J. Q. Chen, *Nucl. Phys. A* **626**, 686 (1997).
- [23] Y. M. Zhao, N. Yoshinaga, S. Yamaji, J. Q. Chen, and A. Arima, *Phys. Rev. C* **62**, 014304 (2000).
- [24] Y. M. Zhao, N. Yoshinaga, S. Yamaji, and A. Arima, *Phys. Rev. C* **62**, 014316 (2000); Y. M. Zhao, A. Arima, J. N. Ginocchio, and N. Yoshinaga, *ibid.* **68**, 044320 (2003).
- [25] T. Takahashi, N. Yoshinaga, and K. Higashiyama, *Phys. Rev. C* **71**, 014305 (2005).
- [26] J. Q. Chen and Y. A. Luo, *Nucl. Phys. A* **639**, 615 (1998); Y. A. Luo and J. Q. Chen, *Phys. Rev. C* **58**, 589 (1998).
- [27] Y. M. Zhao, S. Yamaji, N. Yoshinaga, and A. Arima, *Phys. Rev. C* **62**, 014315 (2000).
- [28] L. Y. Jia, H. Zhang, and Y. M. Zhao, *Phys. Rev. C* **75**, 034307 (2007); **76**, 054305 (2007).
- [29] Z. Y. Xu, Y. Lei, Y. M. Zhao, S. W. Xu, Y. X. Xie, and A. Arima, *Phys. Rev. C* **79**, 054315 (2009).
- [30] H. Jiang, J. J. Shen, Y. M. Zhao, and A. Arima, *J. Phys. G: Nucl. Part. Phys.* **38**, 045103 (2011); H. Jiang, G. J. Fu, Y. M. Zhao, and A. Arima, *Phys. Rev. C* **84**, 034302 (2011).
- [31] <http://www.nndc.bnl.gov/ensdf/>.
- [32] A. Holt, T. Engeland, M. Hjorth-Jensen, and E. Osnes, *Nucl. Phys. A* **634**, 41 (1998).